

## Reversed Crystal-Field Splitting and Spin-Orbital Ordering in $\alpha$ -Sr<sub>2</sub>CrO<sub>4</sub>

Takashi Ishikawa<sup>1</sup>, Tatsuya Toriyama<sup>1</sup>, Takehisa Konishi<sup>2</sup>, Hiroya Sakurai<sup>3</sup>, and Yukinori Ohta<sup>1\*</sup>

<sup>1</sup>*Department of Physics, Chiba University, Chiba 263-8522, Japan*

<sup>2</sup>*Graduate School of Advanced Integration Science, Chiba University, Chiba 263-8522, Japan*

<sup>3</sup>*National Institute for Materials Science, Tsukuba, Ibaraki 305-0044, Japan*

The origin of successive phase transitions observed in the layered perovskite  $\alpha$ -Sr<sub>2</sub>CrO<sub>4</sub> is studied by the density-functional-theory-based electronic structure calculation and mean-field analysis of the proposed low-energy effective model. We find that, despite the fact that the CrO<sub>6</sub> octahedron is elongated along the  $c$ -axis of the crystal structure, the crystal-field level of nondegenerate  $3d_{xy}$  orbitals of the Cr ion is lower in energy than that of doubly degenerate  $3d_{yz}$  and  $3d_{xz}$  orbitals, giving rise to the orbital degrees of freedom in the system with a  $3d^2$  electron configuration. We show that the higher (lower) temperature phase transition is caused by the ordering of the orbital (spin) degrees of freedom.

The orbital degrees of freedom in transition-metal compounds have long been one of the major themes in the physics of strongly correlated electron systems.<sup>1–3)</sup> The simplest example is the cubic perovskite structure, where the transition-metal ion surrounded by six ligand ions forms an octahedron and the corresponding crystal field splits the energy levels of the five  $d$  orbitals into triply degenerate  $t_{2g}$  orbitals and doubly degenerate  $e_g$  orbitals. Moreover, in a layered perovskite with the K<sub>2</sub>NiF<sub>4</sub>-type crystal structure, the octahedron is elongated along the  $c$ -axis and the triply degenerate  $t_{2g}$  levels further split into low-energy doubly degenerate  $d_{xz}$  and  $d_{yz}$  orbitals and the high-energy nondegenerate  $d_{xy}$  orbital.<sup>4)</sup> No one would have doubted this simple law of the crystal field theory.

In this paper, we show that a serious deviation from this simple law occurs in the Mott insulator  $\alpha$ -Sr<sub>2</sub>CrO<sub>4</sub>. This material has the K<sub>2</sub>NiF<sub>4</sub>-type crystal structure with CrO<sub>6</sub> octahedra elongated along the  $c$ -axis and with a  $3d^2$  electron configuration.<sup>5,6)</sup> Therefore, one would naturally expect that two electrons occupy the lowest doubly degenerate  $t_{2g}$  orbitals forming an  $S = 1$  spin due to Hund's rule coupling, so that only the antiferromagnetic Néel ordering of  $S = 1$  spins occurs at the Néel temperature  $T_N$ , without any orbital ordering.<sup>6)</sup> Surprisingly, however, a recent experimental study<sup>7)</sup> revealed that two phase transitions occur successively at 112 and 140 K, releasing nearly the same amount of entropy. The lower-temperature phase transition was ascribed to Néel ordering by magnetic measurement, but the cause of the higher-temperature one (denoted as  $T_S$ ) remains a mystery from the experiment.<sup>7,8)</sup>

In what follows, using the density-functional-theory (DFT)-based electronic structure calculations, we will

show that, in  $\alpha$ -Sr<sub>2</sub>CrO<sub>4</sub>, the crystal-field level of non-degenerate  $3d_{xy}$  orbitals of the Cr ion is in fact lower in energy than that of doubly degenerate  $3d_{yz}$  and  $3d_{xz}$  orbitals. Therefore, in this system with the  $3d^2$  electron configuration, the orbital degrees of freedom are indeed active. More precisely, this system can be modeled as the Kugel-Khomskii-type spin-orbital subsystem<sup>9,10)</sup> consisting of the  $d_{xz}$  and  $d_{yz}$  orbitals of the Cr ion, which couples to the antiferromagnetic Heisenberg subsystem consisting of the  $d_{xy}$  orbitals, via the on-site Hund's ferromagnetic exchange interaction. This description is also justified by the DFT calculation allowing for spin polarization, which predicts the spin- and orbital-ordered ground state in this material. The mean-field analysis of the proposed low-energy effective model, taking into account the Jahn-Teller distortion, can explain the successive phase transitions observed in  $\alpha$ -Sr<sub>2</sub>CrO<sub>4</sub>; i.e., the higher (lower) temperature phase transition is caused by the ordering of the orbital (spin) degrees of freedom. To the best of our knowledge, this is one of the rare examples<sup>11)</sup> of the reversal of the crystal-field levels in transition-metal compounds, which is proved by the solid experimental consequence.

We employ the WIEN2k code<sup>12)</sup> based on the full-potential linearized augmented-plane-wave method for our DFT calculations. We present calculated results obtained in the generalized gradient approximation (GGA) for electron correlations with the exchange-correlation potential of Ref. 13. To improve the description of electron correlations in the Cr  $3d$  orbitals, we use the rotationally invariant version of the GGA+ $U$  method with the double-counting correction in the fully localized limit,<sup>14,15)</sup> where we choose  $U$  to reproduce the band gap observed in experiment. The spin polarization is allowed when necessary. The spin-orbit interaction is not taken

\*ohta@faculty.chiba-u.jp

into account. We use the crystal structure measured at a low temperature,<sup>7)</sup> which has the tetragonal symmetry (space group  $I4/mmm$ ) with the lattice constants  $a = 3.821$  and  $c = 12.492$  in units of Å. There are one (two) crystallographically inequivalent Cr (O) ions. Because no significant structural changes were detected at the phase-transition points,<sup>7)</sup> we assume the same crystal structure for both high- and low-temperature phases, but the unit cell is extended to a  $\sqrt{2} \times \sqrt{2} \times 1$  supercell, allowing for antiferromagnetic spin polarization in the low-temperature phase. In the self-consistent calculations, we use 14850  $\mathbf{k}$ -points in the irreducible part of the Brillouin zone. Muffin-tin radii ( $R_{\text{MT}}$ ) of 2.35 (Sr), 1.88 (Cr), and 1.70 (O) Bohr are used and a plane-wave cutoff of  $K_{\text{max}} = 7.00/R_{\text{MT}}$  is assumed.

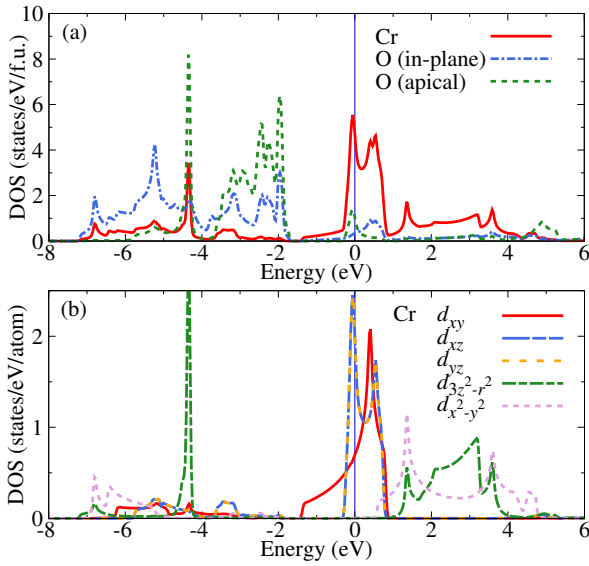


**Fig. 1.** (Color online) (a) Calculated total and partial DOSs (per formula unit, f.u.) in the hypothetical paramagnetic metallic state of  $\alpha$ - $\text{Sr}_2\text{CrO}_4$ . (b) Calculated partial DOSs projected onto the five  $d$  orbitals of Cr. The vertical line in each panel represents the Fermi level.

First, let us discuss the hypothetical paramagnetic metallic phase of  $\alpha$ - $\text{Sr}_2\text{CrO}_4$  obtained under the assumption of no spin polarization. The calculated results for the density of states (DOS) are shown in Fig. 1, where we find that the states near the Fermi level consist mainly of the  $3d$   $t_{2g}$  orbitals of the Cr ion. The orbital-decomposed partial DOSs shown in Fig. 1(b) indicate that the  $3d_{xy}$  orbitals form the skew DOS corresponding to the tight-binding bands of the two-dimensional square lattice and the  $3d_{xz}$  and  $3d_{yz}$  orbitals form the skew DOSs corresponding to those of the one-dimensional chain. The dispersions of the three bands near the Fermi level are shown in Fig. 2(a), which are fitted very well by the tight-binding bands of the three molecular orbitals obtained

as the maximally localized Wannier functions.<sup>16,17)</sup> The shapes of the obtained Wannier functions are illustrated in Fig. 2(b), where we find that the  $d_{xy}$  molecular orbital is composed of the Cr  $3d_{xy}$  atomic orbital with a strong admixture of the  $2p_\pi$  atomic orbitals of the in-plane oxygens O(P). In Fig. 2(c), we also show the  $d_{yz}$  molecular orbital composed of the Cr  $3d_{yz}$  atomic orbital with a strong admixture of the  $2p_z$  atomic orbitals of O(P) and  $2p_y$  atomic orbitals of apical oxygen O(A).

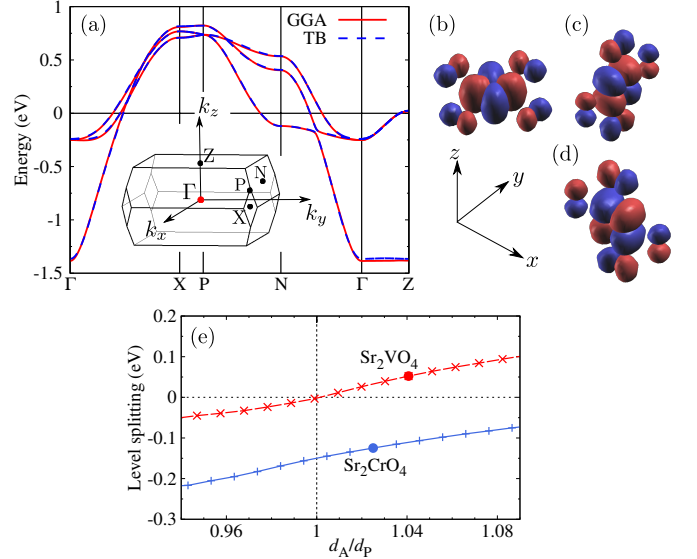


**Fig. 2.** (Color online) (a) Calculated band dispersions near the Fermi level compared with the tight-binding bands of the maximally localized Wannier orbitals. The horizontal line indicates the Fermi level. The inset shows the Brillouin zone. (b) Illustration of the maximally localized Wannier functions for the  $3d_{xy}$  orbital of Cr admixed with the  $2p_x$  and  $2p_y$  orbitals of O(P). (c) Same as in (b) but for the  $3d_{yz}$  orbital admixed with  $2p_z$  of O(P) and  $2p_y$  of O(A). (d) Same as in (c) but for the  $3d_{xz}$  orbital. (e) Calculated energy-level splitting  $\varepsilon(d_{xy}) - \varepsilon(d_{yz})$  of the maximally localized Wannier orbitals as a function of  $d_A/d_P$ . The results for  $\text{Sr}_2\text{VO}_4$  are also shown for comparison. The dots indicate the results obtained for the experimental bond lengths.

From the above tight-binding fitting, we derive the crystal-field levels of the  $t_{2g}$  orbitals. The obtained energy-level splitting between the  $d_{xy}$  molecular orbital and the  $d_{xz}$  and  $d_{yz}$  molecular orbitals is shown in Fig. 2(e) as a function of the distance  $d_A$  between the Cr and O(A) ions divided by the distance  $d_P$  between the Cr and O(P) ions. The splitting is calculated by shifting only the positions of O(A) ions from the experimental position. The results of  $\alpha$ - $\text{Sr}_2\text{VO}_4$  are also shown for comparison. We find here that indeed the crystal-field levels are reversed in  $\alpha$ - $\text{Sr}_2\text{CrO}_4$ , regardless of the elongation of the  $\text{CrO}_6$  octahedron examined, which is in sharp contrast to the case of  $\alpha$ - $\text{Sr}_2\text{VO}_4$ .<sup>18–20)</sup> We also examined the electronic state of  $\text{LaSrVO}_4$ , which has the same crystal

structure with the  $3d^2$  electron configuration,<sup>21,22</sup> only the antiferromagnetic phase transition was observed experimentally.<sup>8,23</sup> Our DFT calculation shows that the reversal of the crystal-field levels does not occur in this material.

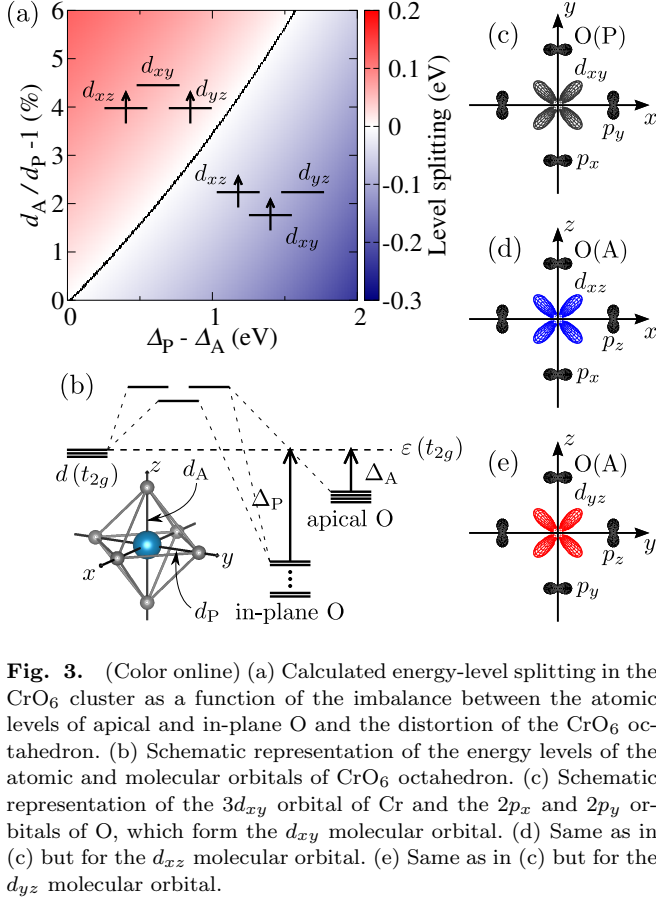


**Fig. 3.** (Color online) (a) Calculated energy-level splitting in the  $\text{CrO}_6$  cluster as a function of the imbalance between the atomic levels of apical and in-plane O and the distortion of the  $\text{CrO}_6$  octahedron. (b) Schematic representation of the energy levels of the atomic and molecular orbitals of  $\text{CrO}_6$  octahedron. (c) Schematic representation of the  $3d_{xy}$  orbital of Cr and the  $2p_x$  and  $2p_y$  orbitals of O, which form the  $d_{xy}$  molecular orbital. (d) Same as in (c) but for the  $d_{xz}$  molecular orbital. (e) Same as in (c) but for the  $d_{yz}$  molecular orbital.

The origin of this reversal of the crystal-field levels manifests itself in the energy levels of the  $\text{CrO}_6$  cluster. Here, we take into account the three  $t_{2g}$  atomic orbitals of Cr and twelve  $2p$  atomic orbitals of O(P) and O(A), which are linked by  $\pi$  bonds. The  $e_g$  atomic orbitals and  $2p$  atomic orbitals linked by  $\sigma$  bonds, which are orthogonal to the  $t_{2g}$  orbitals, are neglected. The energy levels of these atomic orbitals, together with the energy levels of molecular orbitals as the antibonding orbitals of the  $t_{2g}$  and  $2p$  atomic orbitals, are defined in Fig. 3(b); in particular, we define the level differences  $\Delta_A = \varepsilon(t_{2g}) - \varepsilon(\text{O(A)})$  and  $\Delta_P = \varepsilon(t_{2g}) - \varepsilon(\text{O(P)})$ . The calculated results for the crystal-field splitting are shown in Fig. 3(a), where we find that the imbalance between the atomic levels of O(A) and O(P), as well as the distortion of the  $\text{CrO}_6$  octahedron, plays an essential role. The energy level of the atomic  $2p$  orbitals of O(A) shifts upward and approaches the energy levels of the  $t_{2g}$  atomic

orbital, just as in the negative charge-transfer-gap situation<sup>24,25</sup> occurring in, e.g.,  $\text{CrO}_2$ <sup>26</sup> and  $\text{K}_2\text{Cr}_8\text{O}_{16}$ ,<sup>27,28</sup> which causes the reversal of the crystal-field levels.

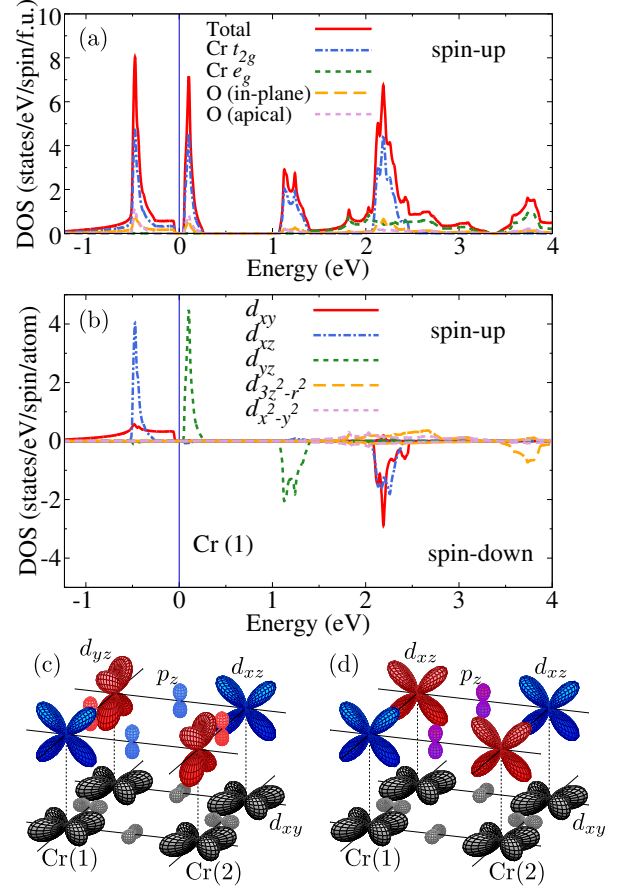


**Fig. 4.** (Color online) Calculated (a) total and (b) orbital-decomposed partial DOSs in the antiferromagnetic phase of  $\alpha\text{-Sr}_2\text{CrO}_4$ . The vertical line indicates the Fermi level.  $U = 0.9$  eV is assumed. (c) Schematic representation of the ground-state spin-orbital ordering pattern in  $\alpha\text{-Sr}_2\text{CrO}_4$ . Note that the  $d_{xz}$  and  $d_{yz}$  orbitals are illustrated separately from the  $d_{xy}$  orbitals. (d) Same as in (c) but for the second lowest energy state.

Next, let us discuss the symmetry-broken ground state of  $\alpha\text{-Sr}_2\text{CrO}_4$ . We carry out the DFT calculation allowing for spin polarization using the GGA+ $U$  approach. The calculated results are shown in Fig. 4, where we find that the spin- and orbital-ordered ground state is actually realized; i.e., the  $3d_{xy}$  orbitals are always occupied by one electron, but either the  $d_{xz}$  or  $d_{yz}$  orbital is occupied by one electron, leading to orbital ordering. This result reinforces the concept of the reversed crystal-field levels in  $\alpha\text{-Sr}_2\text{CrO}_4$  discussed above. The calculated spatial pattern indicates that the spin degrees of freedom show the spin  $S = 1$  antiferromagnetic Néel ordering as expected, but the orbital degrees of freedom also show antiferro ordering, which is not expected from the Kugel-Khomskii

theory.<sup>9,10)</sup> However, we find that the spin-antiferro and orbital-ferro state also appears as a metastable state with the second lowest energy; the energy difference is only 0.02122 eV/f.u. There might be other low-energy orbital ordering patterns if we use larger supercells; the real pattern should eventually be determined experimentally.

We also find that the energy gap appears in the calculated DOS curves (see Fig. 4), so that the system is insulating in agreement with the experiment where the band gaps of 0.10 eV (from the resistivity of a bulk sample)<sup>7)</sup> and  $\sim 0.3$  eV (from optical measurement on a thin film)<sup>29)</sup> were reported.  $U$  can be adjusted to reproduce such band gaps without any significant changes in our discussion.

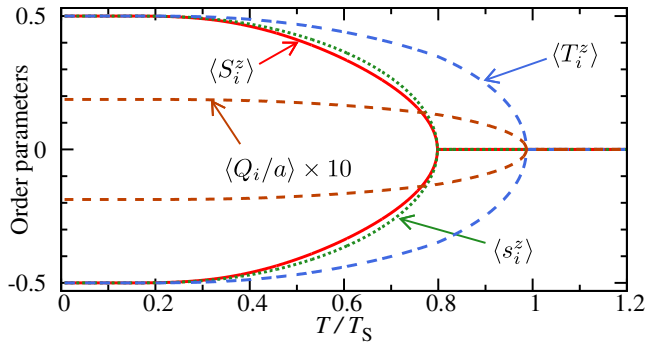


**Fig. 5.** (Color online) Temperature dependence of the order parameters calculated in the mean-field approximation for our effective model. The parameter values used are  $K = 0.05$ ,  $J_{AF} = 0.1$ ,  $J_H = 0.5$ ,  $ga = 15$ ,  $ka^2 = 2500$ , and  $\lambda a^2 = 525$  in units of eV, which result in  $T_S = 1390$  K and  $T_N = 1110$  K.

Finally, let us discuss the low-energy effective model describing the spin and orbital orderings in  $\alpha$ - $\text{Sr}_2\text{CrO}_4$ . This model represents the two-dimensional  $\text{CrO}_4$  plane made of (i) the Kugel-Khomskii subsystem consisting of the Cr  $3d_{xz}$  and  $3d_{yz}$  orbitals (hybridized with O  $2p$  orbitals), leading to the orbital ordering, (ii) the antiferromagnetic Heisenberg subsystem consisting of the  $3d_{xy}$  orbital (hybridized with O  $2p$  orbitals), leading to the robust antiferromagnetic background, (iii) the Hund's ferromagnetic exchange interaction acting between the electron on the  $3d_{xy}$  orbital and electron on the  $3d_{xz}$  or  $3d_{yz}$  orbital in the same Cr site, and (iv) the Jahn-Teller coupling with the lattice degrees of freedom. This model in the strong-coupling version may be defined by the Hamiltonian

$$\mathcal{H}_{\text{eff}} = K \sum_{\langle ij \rangle} \left( 2\mathbf{S}_i \cdot \mathbf{S}_j + \frac{1}{2} \right) \left( 2\mathbf{T}_i \cdot \mathbf{T}_j + \frac{1}{2} \right) + J_{AF} \sum_{\langle ij \rangle} \mathbf{s}_i \cdot \mathbf{s}_j - J_H \sum_i \mathbf{S}_i \cdot \mathbf{s}_i$$

$$+ g \sum_i Q_i T_i^z + \frac{k}{2} \sum_i Q_i^2 + \lambda \sum_{\langle ij \rangle} Q_i Q_j, \quad (1)$$

where the first term represents the Kugel-Khomskii interaction  $K$  between the spins  $\mathbf{S}_{i,j}$  and the pseudospins  $\mathbf{T}_{i,j}$  in the  $d_{xz}$  and  $d_{yz}$  orbitals in the nearest-neighbor sites  $\langle ij \rangle$ ; the second and third terms represent the Heisenberg exchange interaction  $J_{AF}$  between the two spins  $\mathbf{s}_i$  and  $\mathbf{s}_j$  in the  $d_{xy}$  orbitals and the Hund's ferromagnetic exchange interaction  $J_H$ , respectively. The terms in the last line of Eq. (1) represent the Jahn-Teller coupling between the pseudospin and the lattice degrees of freedom written in terms of the normal coordinates of the lattice distortion  $Q_i$ .

We analyze this model using the semiclassical mean-field approximation,<sup>4)</sup> taking  $\langle S_i^z \rangle$ ,  $\langle T_i^z \rangle$ ,  $\langle s_i^z \rangle$ , and  $\langle Q_i \rangle$  to be the order parameters, where we again assume the extended unit cell of  $\sqrt{2} \times \sqrt{2}$ . The results for the temperature dependence of the order parameters are shown in Fig. 5, where we find that the successive phase transitions are well reproduced, i.e., the ordering of the pseudospins occurs at  $T_S$ , which is followed by the ordering of the spins at  $T_N$ , just as in the experiment.<sup>7)</sup> The obtained large  $T_S$  and  $T_N$  are due to the insufficiency of the mean-field approximation, where the strong quantum fluctuations of the two-dimensional spin system are completely neglected.

In summary, using the DFT-based electronic structure calculations and effective model analysis, we have elucidated the origin of the successive phase transitions observed in a layered perovskite  $\alpha$ - $\text{Sr}_2\text{CrO}_4$ . We showed that the crystal-field level of nondegenerate  $3d_{xy}$  orbitals of the Cr ion is lower in energy than that of doubly degenerate  $3d_{yz}$  and  $3d_{xz}$  orbitals, despite the fact that the  $\text{CrO}_6$  octahedron is elongated along the  $c$ -axis of the crystal structure, which gives rise to the orbital degrees of freedom in the system with a  $3d^2$  electron configuration. This is one of the rare examples of the reversal of crystal-field splitting. We obtained the spin- and orbital-ordered ground state by DFT calculations allowing for spin polarization. We proposed the low-energy effective model made of the Kugel-Khomskii-type spin-orbital subsystem consisting of the  $d_{xz}$  and  $d_{yz}$  orbitals of the Cr ion and the antiferromagnetic Heisenberg subsystem consisting of the  $d_{xy}$  orbitals, which are coupled via the on-site Hund's ferromagnetic exchange interaction, together with the Jahn-Teller distortion. The mean-field calculation of this model was shown to account for the observed successive phase transitions. We showed that the imbalance between the atomic energy levels of the in-plane and apical oxygens, as well as the distortion of the  $\text{CrO}_6$  octahedra, plays an essential role in the reversal of the crystal-field levels.

We hope that our work presented here will encourage further experimental studies, such as the direct confirmation of the presence of orbital ordering and the de-

termination of its spatial pattern, as well as the precise determination of the low-temperature crystal structure.

**Acknowledgment** We thank M. Itoh and Y. Ueda for enlightening discussions. This work was supported in part by Futaba Electronics Memorial Foundation and by a Grant-in-Aid for Scientific Research (No. 26400349) from JSPS of Japan. T.T. acknowledges the support from the JSPS Research Fellowship for Young Scientists.

- 1) D. I. Khomskii, *Transition Metal Compounds* (Cambridge University Press, Cambridge, England, 2014).
- 2) Y. Tokura and N. Nagaosa, *Science* **288**, 462 (2000).
- 3) M. Imada, A. Fujimori, and Y. Tokura, *Rev. Mod. Phys.* **70**, 1039 (1998).
- 4) P. Fazekas, *Lecture Notes on Electron Correlation and Magnetism* (World Scientific, Singapore, 1999).
- 5) J. A. Kafalas and J. M. Longo, *J. Solid State Chem.* **4**, 55 (1972).
- 6) T. Baikie, Z. Ahmad, M. Srinivasan, A. Maignan, S. S. Praman, and T. J. Whitea, *J. Solid State Chem.* **180**, 1538 (2007).
- 7) H. Sakurai, *J. Phys. Soc. Jpn.* **83**, 123701 (2014).
- 8) J. Sugiyama, H. Nozaki, I. Umegaki, W. Higemoto, E. J. Ansaldo, J. H. Brewer, H. Sakurai, T.-H. Kao, H.-D. Yang, and M. Månsson, *J. Phys.: Conf. Ser.* **551**, 012011 (2014).
- 9) K. I. Kugel and D. I. Khomskii, *Sov. Phys. JETP* **37**, 725 (1973).
- 10) K. I. Kugel and D. I. Khomskii, *Sov. Phys. Usp.* **25**, 231 (1982).
- 11) Another example is the spinel compound  $\text{LiV}_2\text{O}_4$ , where the  $t_{2g}$  levels of the V ion split into a lower-energy  $a_{1g}$  level and higher-energy doubly-degenerate  $e'_g$  levels due to a threefold local crystal field, despite the fact that the oxygen octahedra are elongated along the local [111] axes. See J. Matsuno, A. Fujimori, and L. F. Mattheiss, *Phys. Rev. B* **60**, 1607 (1999).
- 12) P. Blaha, K. Schwarz, G. K. H. Madsen, D. Kvasnicka, and J. Luitz, *Wien2k, An Augmented Plane Wave Plus Local Orbitals Program for Calculating Crystal Properties* (Technische Universität Wien, Austria, 2001).
- 13) J. P. Perdew, K. Burke, and M. Ernzerhof, *Phys. Rev. Lett.* **77**, 3865 (1996).
- 14) V. I. Anisimov, I. V. Solovyev, M. A. Korotin, M. T. Czyżyk, and G. A. Sawatzky, *Phys. Rev. B* **48**, 16929 (1993).
- 15) A. I. Liechtenstein, V. I. Anisimov, and J. Zaanen, *Phys. Rev. B* **52**, R5467 (1995).
- 16) A. A. Mostofi, J. R. Yates, Y.-S. Lee, I. Souza, D. Vanderbilt, and N. Marzari, *Comp. Phys. Commun.* **178**, 685 (2008).
- 17) J. Kunes, R. Arita, P. Wissgott, A. Toschi, H. Ikeda, and K. Held, *Comp. Phys. Commun.* **181**, 1888 (2010).
- 18) Y. Imai, I. V. Solovyev, and M. Imada, *Phys. Rev. Lett.* **95**, 176405 (2005).
- 19) H. D. Zhou, B. S. Conner, L. Balicas, and C. R. Wiebe, *Phys. Rev. Lett.* **99**, 136403 (2007).
- 20) J. Sugiyama, H. Nozaki, I. Umegaki, W. Higemoto, E. J. Ansaldo, J. H. Brewer, H. Sakurai, T.-H. Kao, H.-D. Yang, and M. Månsson, *Phys. Rev. B* **89**, 020402(R) (2014).
- 21) J. E. Greedan and W. Gong, *J. Alloys Compd.* **180**, 281 (1992).
- 22) J. M. Longo and P. M. Raccach, *J. Solid State Chem.* **6**, 526 (1973).
- 23) Z. L. Dun, V. O. Garlea, C. Yu, Y. Ren, E. S. Choi, H. M. Zhang, S. Dong, and H. D. Zhou, *Phys. Rev. B* **89**, 235131 (2014).
- 24) J. Zaanen, G. A. Sawatzky, and J. W. Allen, *Phys. Rev. Lett.* **55**, 418 (1985).
- 25) D. I. Khomskii, *Lithuanian J. Phys.* **37**, 2001 (1997); arXiv:cond-mat/0101164.
- 26) M. A. Korotin, V. I. Anisimov, D. I. Khomskii, and G. A. Sawatzky, *Phys. Rev. Lett.* **80**, 4305 (1998).
- 27) T. Toriyama, A. Nakao, Y. Yamaki, H. Nakao, Y. Murakami, K. Hasegawa, M. Isobe, Y. Ueda, A. V. Ushakov, D. I. Khomskii, S. V. Streltsov, T. Konishi, and Y. Ohta, *Phys. Rev. Lett.* **107**, 266402 (2011).
- 28) M. Sakamaki, T. Konishi, and Y. Ohta, *Phys. Rev. B* **80**, 024416 (2009); **82**, 099903(E) (2010).
- 29) J. Matsuno, Y. Okimoto, M. Kawasaki, and Y. Tokura, *Phys. Rev. Lett.* **95**, 176404 (2005).